Electronic Properties of MoS₂ Nanoparticles

Tianshu Li and Giulia Galli*

Department of Chemistry, University of California, Davis, California 95616

Received: July 11, 2007; In Final Form: August 14, 2007

We present a first principle, theoretical study of MoS₂ nanoparticles that provides a unified explanation of measured photoluminescence spectra and recent STM measurements as a function of size. In addition, our calculations suggest ways to engineer the electronic properties of these systems so as to obtain direct band gap 3D layered nanoparticles or Mo doped metallic nanowires. In particular, we show that single sheet MoS₂ nanoparticles up to ∼3.4 nm show no appreciable quantum confinement effects. Instead, their electronic structure is entirely dominated by surface states near the Fermi level. In 3D nanoparticles, we found a strong dependence of their electronic properties on layer stacking and distance, and we suggest that the observed photoluminescence variation as a function of size originates from the number of planes composing the system. The number of these planes and their distance can be tuned to engineer clusters with direct band gaps, at variance with the bulk. Our results also suggest ways to take advantage of surface states to design metallic nanowires with novel catalytic and thermoelectric properties.

1. Introduction

Molybdenum disulfide nanostructures are receiving considerable attention because of their potential applications as catalysts for desulfurization processes[1] and hydrogen evolution,[2,3] as well as promising materials for thermoelectric applications, similar to tungsten diselenides.[4] In addition, hollow MoS₂ nanoparticles have shown very promising tribological applications, exhibiting ultralow friction and wear properties under certain preparation conditions.[5,6]

Several years ago it was shown that MoS₂ nanoplatelets smaller than 3 nm, and consisting of only one S−Mo−S layer, may be synthesized.[7] Scanning tunneling microscopy (STM) experiments[7] combined with density functional theory (DFT) calculations[8−10] have revealed that these platelets, deposited on Au(111), have a distinct triangular shape. Intriguingly, these nanoparticles appeared to have metallic edge states,[8] that is, they exhibit electronic properties quite different from their bulk counterpart, an indirect band gap semiconductor. The Mo_xS_y clusters up to ∼100 atoms can also be obtained in the gas phase,[11−14] and DFT studies suggested the existence of magic number structures[15,16] and the tendency for stabilization of the platelet structures with increasing size.[14,15]

However, previous studies[17,18] reported a semiconducting behavior for MoS₂ nanoparticles, in particular, optical absorption spectra blue-shifted with respect to that of the bulk, to indicate quantum confinement effects as the cluster size is reduced. The in-plane size reduction was assumed to be responsible for the observed confinement, but the particle surface structures could not be investigated, because of insufficient resolution in TEM images.

A very recent STM experiment[1] has detected a clear size dependence of the morphology and electronic structure of MoS₂ triangular platelets. Interestingly, the size distribution of these nanoparticles showed a dependence on the number of sulfur atoms present on the edge. In low bias STM experiments, large

clusters with an even number of S dimers yielded higher statistical counts than those with an odd sequence. This observation has been rationalized in terms of sulfur pairing on the edge, which would be energetically favored only for certain sizes of the platelets.

With the goal of understanding the electronic properties of MoS₂ nano particles, especially their size dependence and edge structure and their influence on catalytic activity, we carried out ab initio calculations of two- and three-dimensional (2D and 3D, respectively) MoS₂ nanoparticles up to 3.4 nm in lateral dimensions. Our results provide a unified explanation of recently observed STM images as a function of size and of photoluminescence data. In addition, our findings suggest a way to engineer 3D semiconducting MoS₂ nanoparticles with direct band gaps, as well as metallic, dichalcogenides nanowires with promising catalytic and thermoelectric properties. The rest of the paper is organized as follow: In Section 2 we give computational details, and in Section 3 we present and discuss our results. Our conclusions are reported in Section 4.

2. Computational Details

The structure of bulk 2H-MoS₂ is similar to that of graphite: it consists of S−Mo−S layers arranged with *ABAB* stacking and bound by weak, van der Waals type interactions. The MoS₂ nanoplatelets are portions of bulk layers and may display various edge geometries. To model these nanoparticles, we assumed triangular shapes, following the experimental data reported in ref 7, and we considered three different edge structures, that is, (i) a Mo edge with 100% S coverage, (ii) a Mo edge with 50% S coverage, and (iii) a S edge with 100% S coverage. As shown in Figure 1, in all configurations, bonds involving Mo atoms are fully saturated. We characterize a given cluster by the number (*N*) of Mo atoms on one edge of the particle. In our study, we considered clusters with *N* up to 12 (side length up to 3.4 nm).

We carried out first principles calculations using DFT in the generalized gradient approximation (GGA PW91) with the PWscf package.[19] We employed plane wave basis sets and

* To whom correspondence should be addressed. E-mail: gagalli@ucdavis.edu.

Electronic Properties of MoS$_2$ Nanoparticles

J. Phys. Chem. C, Vol. 111, No. 44, 2007 **16193**
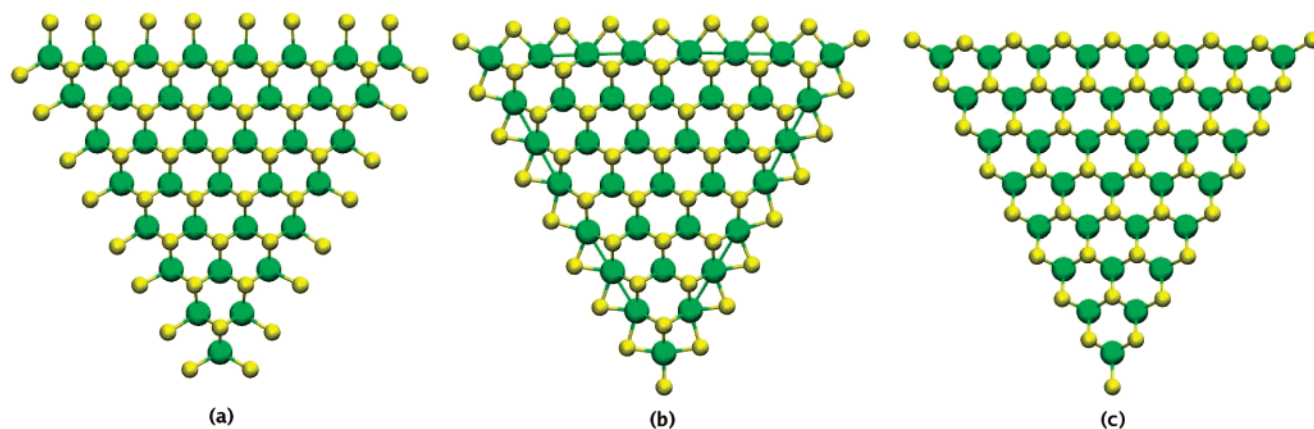
Figure 1. Top view of MoS$_2$ triangular nano clusters in the geometries obtained in our ab initio calculations. The Mo and S atoms are represented by green and yellow spheres, respectively. (a) Mo edge terminated by S dimers (100% S coverage), S atoms bonded to Mo form dimer pairs ($\sim$2 Å) normal to the basal plane. The neighbor S dimers further pair up along the edge direction, giving rise to a double periodicity relative to the hexagonal lattice of the bulk. (b) Mo edge terminated by S monomers (50% S coverage), where each S monomer is shared by two adjacent Mo atoms on the edge. Upon relaxation, three edge Mo atoms form a trimer, creating a superstructure with periodicity corresponding to three times that of the bulk lattice constant. (c) S edge terminated by S dimers (100% coverage). The S adatoms were found to dimerize along the direction normal to the basal plane, but their bond length ($\sim$2.86 Å) is larger than that of S dimers in structure (a). In (c), no superstructure was generated upon atomic relaxation.

ultrasoft pseudopotentials,[20] with cutoff energies of 30 and 250 Ry for wavefunctions and charge density, respectively. Nanoparticles were placed in supercells large enough to allow for a 10 Å distance between periodic replica. Occupation numbers of single particle electronic states were determined using the cold smearing method[21] with a smearing width of 0.04Ry. For each configuration, atomic positions were fully relaxed until the force acting on each atom was less than 0.05 eV/Å.

Upon full atomic relaxation of all structures, we found that the bond lengths of the core atoms of all clusters remain nearly unchanged relative to the corresponding ones in the bulk, for example, both Mo$-$S and Mo$-$Mo bond lengths decrease by less than 0.01 Å. Structural rearrangements or reconstructions are instead observed on the edge of the nanoparticles, and they are reported in Figure 1.

3. Results and Discussion

The excess sulfur atoms on the cluster edge make the S/Mo ratio of all platelets larger than the bulk value of 2, and this ratio increases steeply as the cluster size decreases. The excess S atoms introduce p states with energies comparable to the p$-$d hybridized states near the top of valence band. Therefore the electronic states localized on the nanoparticle edges, particularly from the outermost S and Mo atomic rings, have energies close to the Fermi level, and they determine the conduction properties of the system. For N values larger than 6 (side length greater than 1.55 Å), clusters with 100% S coverage, with both Mo edge and S edge, show metallic-like behavior, namely no clear energy gap is observed (given the smearing function used here), whereas the 50% covered Mo edge always exhibits a small gap ($\sim$0.6 eV). This behavior can be generally understood on the basis of the degree of sulfur excess; for clusters with the same size N, 50% S coverage yields the S/Mo ratio ($= 2 + 2/(N + 1)$) closer to 2 than the 100% coverage ($2 + 8/(N + 1)$) and $2 + 4/N$ for Mo edge and S edges, respectively), thus introducing much fewer edge states to fill in the energy gap. Interestingly, we also observed a subtle, however discernible, parity dependence of the calculated density of states near the Fermi level in Mo edge covered by 100% S. We suggest that this is related to the trend observed in STM images of MoS$_2$ nanoparticles as a function of size, as we discuss below.
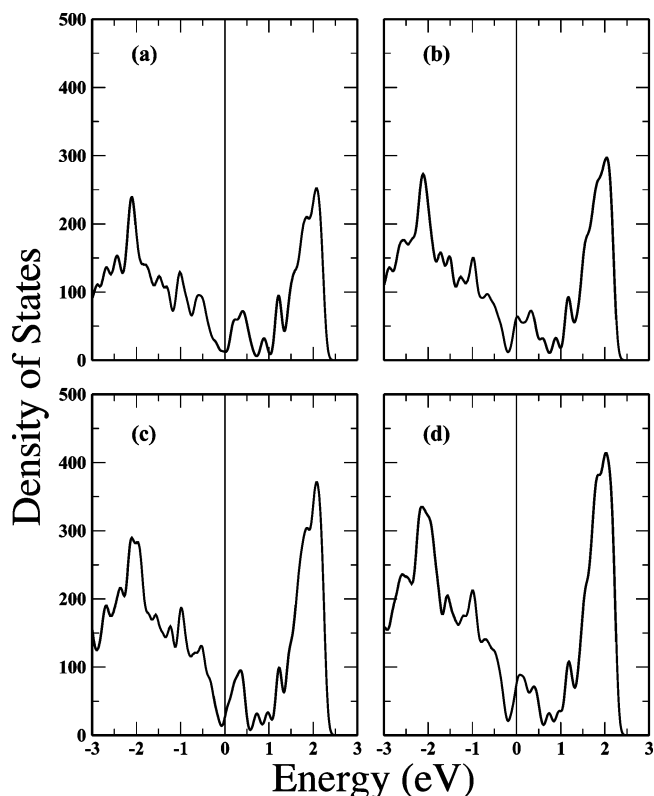
Figure 2. Local density of electronic states (LDOS) in the vicinity of the Fermi level for MoS$_2$ nanoparticles with the Mo edge terminated by 100% S (see Figure 1 a). When N is odd (i.e., in panel (a), $N = 9$ for Mo$_{45}$S$_{126}$ and in panel (c), $N = 11$ for Mo$_{66}$S$_{176}$), we observe a dip in LDOS at the Fermi level, whereas when N is even (e.g., in panel (b), $N = 10$ for Mo$_{55}$S$_{150}$ and in panel (d), $N = 12$ for Mo$_{78}$S$_{204}$) we observe a maximum. This is a general pattern found for all of the clusters with this edge structure. The electronic states presented here are Gaussian broadened by 0.1 eV.

For clusters with even N values of Mo atoms (see Figure 2, panels b and d), the Fermi level resides near a local maximum in the electronic density of states (EDOS), whereas for odd N values (Figure 2, panels a and c), the Fermi level sits in a local valley. Although all of these clusters are metallic-like, this difference in EDOS near E_F may lead to observable differences
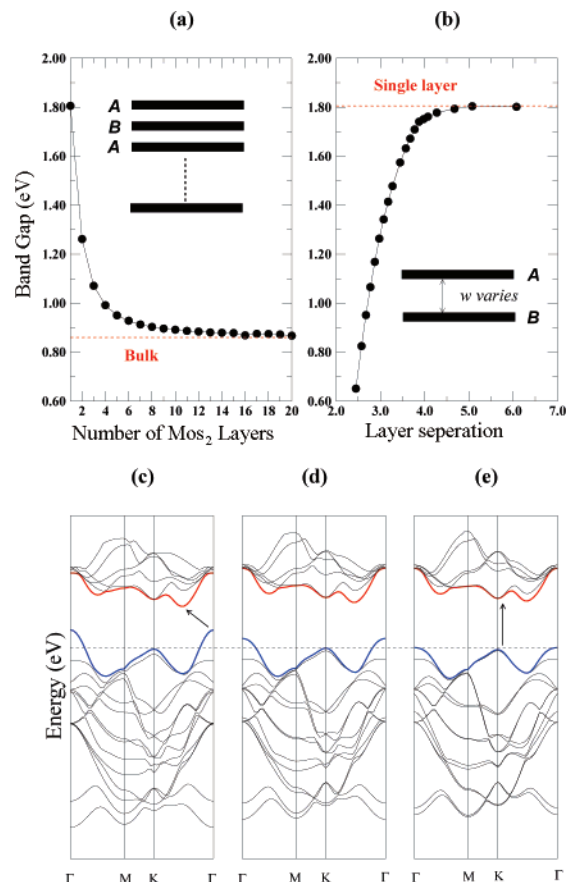
(a)
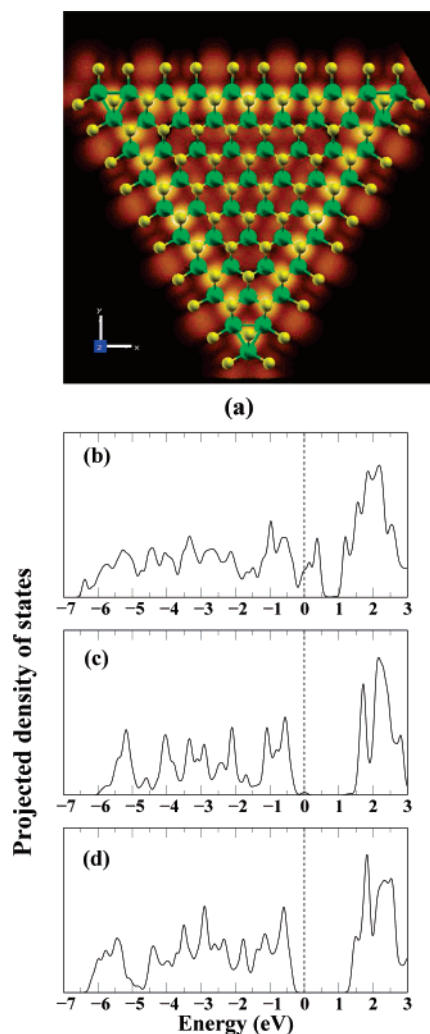
Figure 3. (a) Simulated STM image of $Mo_{55}S_{150}$ (see text). Panels (b) and (c) show the PDOS on the outermost Mo triangular ring and on the center Mo atom, respectively, for the cluster displayed in panel (a). As a comparison, a PDOS of Mo in the single layer MoS_2 sheet is given in panel (d).

Figure 4. Variations of the band gap in multilayer MoS_2 sheets with respect to (a) the number of sheets n and (b) separation distance w, where w refers to the z-axis distance between the upper S layer of sheet B and the lower S layer of sheet A. Note that both sheets A and B contain three atomic layers S−Mo−S. The band structure shown in panels (c−e) correspond to calculations reported in panel (b) and to the separations w = 2.58Å, 2.98Å, and 3.58Å, respectively. For comparison, the eigen energies are aligned with respect to the valence band top at the K-point.

in STM images. Indeed, to first-order, a constant current STM image is representative of the EDOS at the Fermi level. Therefore, on the basis of our results, we expect an alternate bright/dark pattern as a function of N in low bias STM experiments. This is precisely what has been observed in ref 1, where the authors were able to experimentally monitor the finest details of the electronic structure of MoS_2 nanoparticles.

In particular, we found that different edge structures as a function of size are responsible for different density of states at the Fermi level. When the number of edge S dimers is even, all of the edge sulfur atoms participate in pairing, and edge superstructures are formed with a double period. The double period structure is disrupted when N is odd, and lone-paired S atoms are present. For perfectly paired sulfur atoms, a maximum of EDOS is observed at the Fermi level, which makes these particles more visible in STM images, whereas for edge structure with lone pair atoms, a lower density of states at the Fermi level is detected.

To make direct contact with experiment, we computed STM images corresponding to computationally optimized structures using the Tersoff−Hamann[22] approximation. In agreement with ref 1, simulated STM images (Figure 3a) show two salient features: a bright brim across the triangle edge and central protrusions out of registry of S dimers. These were found to

originate from d states localized on the outermost Mo row, and from p_x orbitals localized in the interstitial regions between S dimers. Similar features have been identified in prior studies of infinitely long MoS_2 nanoslabs as "one-dimensional metallic edge states".[8] In finite nanoparticles, however, the edge structure is slightly modified with respect to the infinite slab. For example, it is energetically more favorable for adjacent S dimers to form pairs, which are accompanied by an overlap between antibonding p_x orbitals. As a consequence, the electronic density is decreased in between and increased outside the paired S dimers, and a series of alternate bright/dark protrusions are seen along the particle edge in STM images. These features are unique to the finite clusters terminated with Mo edge covered by 100% S dimers.

We have seen so far that the edge atomic structure plays a key role in determining the electronic properties of 2D MoS_2 nanoparticles, and we now turn to the study of the influence of core states on the properties of these systems, with emphasis on the question of possible quantum confinement effects that were suggested in refs 17 and 18. To this end, we have calculated the projected density of states (PDOS) on each triangular ring of the nanoplatelets. It is seen from Figure 3 that edge states appearing in the vicinity of the Fermi level are mostly localized on the two outermost atomic rings and that the states localized in the core of the cluster are essentially bulk-like. The magnitude of the energy gap between occupied and

Electronic Properties of MoS$_2$ Nanoparticles

J. Phys. Chem. C, Vol. 111, No. 44, 2007 **16195**
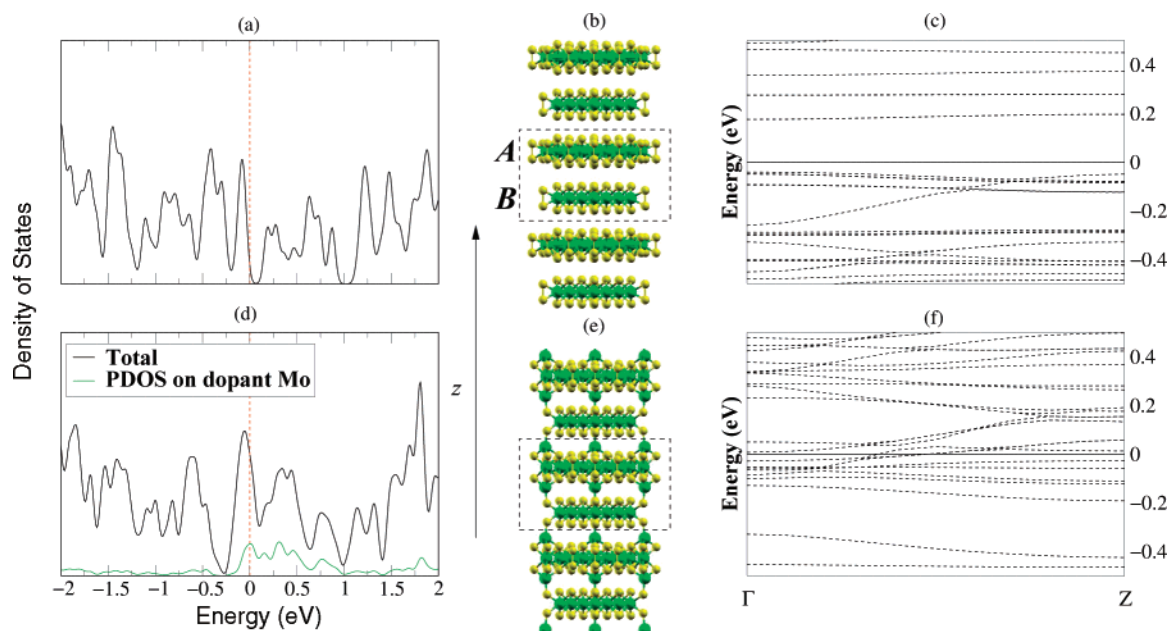
Figure 5. (a) EDOS of MoS$_2$ nanowires built by stacking two triangular single layer clusters alternatively along the *z*-axis, as shown in panel (b). The two building blocks are: *A* (Mo$_{15}$S$_{50}$, Mo edge terminated with S dimers, $N = 5$) and *B* (Mo$_{10}$S$_{30}$, S edge terminated with S dimers, $N = 4$). The dash rectangle shows the unit cell. Panel (c) gives the band structure of the geometry shown in panel (b) along the *z*-axis ($\Gamma \rightarrow Z$). In panel (e), three Mo atoms are intercalated between *A* and *B* at the three corners of the triangle. Each Mo adatom is tetrahedrally coordinated. The corresponding EDOS and band structure are shown in panels (d) and (f), respectively. For all EDOS and band structures, the Fermi energy is set to zero. The electronic states in EDOS are Gaussian broadened by 0.05 eV.

empty core-like states (i.e., electronic states localized in the cluster core) is basically constant as the cluster size is varied, and it equals the value (~1.7 eV) found for an infinite, single MoS$_2$ sheet. Therefore, we conclude that no noticeable quantum confinement effects are present in MoS$_2$ nanoplatelets, even for very small sizes (~2 nm), as opposed to 3D semiconductor nanoparticles. This is consistent with estimates of the exciton radius for bulk MoS$_2$, which is about 2.0 nm.[23] For a pseudo-2D system, this radius is expected to be even smaller,[24] and thus quantum confinement effects are unlikely for sizes larger than 1−2 nm.

Our results indicate that the blue shift observed experimentally in photoluminescence spectra[17] does not originate from confinement within the *xy* plane. We show in the following that it is instead present when 3D MoS$_2$ nanoparticles composed of several layers are considered.

We investigated possible size effects on the calculated electronic HOMO−LUMO gap, when varying the number of sheets (*n*) and the sheets separation distance (*w*, see Figure 4), respectively. In the former case, infinite-wide single S−Mo−S sheets are stacked with *ABA* sequence while keeping the inter-sheet distance *w* fixed to the bulk value. The calculated band gap, as illustrated in Figure 4a, monotonically decreases from 1.8 to 0.86 eV as *n* increases from 1 to infinity. As for the latter case, only two such single sheets are stacked as A and B, but their distance *w* is varied. As a result, the band gap increases monotonically with *w* (Figure 4b). When the inter-sheet separation is greater than 4.5 Å, the gap reaches the value found for a single sheet, as the inter-sheet interaction vanishes.

To understand the observed strong dependence of MoS$_2$ particle electronic structure on the separation distance, we examined in detail the variation of the band structure with respect to separation distance *w* between two sheets. As shown in Figure 4, panels c−e, significant changes take place at the top of the valence band. Specifically, the energies of the single particle states near the Γ point drop substantially as *w* increases. These states originate from a linear combination of p$_z$ orbitals

on S atoms and d$_{z^2}$ orbitals on Mo atoms,[25] both of which are rather delocalized and have an antibonding nature. When the interlayer distance increases and the layer−layer interaction decreases, then the energy arising from antibonding states is lowered. On the other hand, both the top of the valence band and the bottom of the conduction band near the *K*-point are primarily composed of orbitals localized in the *xy* plane, and these basically are unaffected by a change of distance along *z*. Such a downward energy shift at Γ not only results into an increase of the band gap but changes its nature from indirect (as in the bulk) to direct. This change in character presents an interesting opportunity for engineering the electronic properties of layered MoS$_2$ composites as a function of interlayer separation and/or number of layers.

Finally, we suggest a way to engineer metallic MoS$_2$ nanowires that could have promising applications as thermoelectric materials. Transition metal dichalcogenides are known to be poor electric and thermal conductors across the MoS$_2$ planes, and as semiconducting materials, in principle, they may not appear to be good candidates for high figure of merit thermoelectrics. However, a very low thermal conductivity in the *z*-direction was recently reported[4] for disordered WSe$_2$ thin films, which are similar to MoS$_2$ in structure and bonding. This conductivity is the lowest ever measured for a solid. It is therefore of great interest to explore possible ways to increase the electrical conductivity of transition metal dichalcogenides, with the goal of engineering high figure of merit materials for thermoelectric applications. Building conducting 3D wires is also of interest for catalytic applications involving these materials. Here we propose that MoS$_2$ nanowires with Mo atoms intercalated within MoS$_2$ planes may exhibit a metallic-like behavior and thus become conducting.

We considered two single layer MoS$_2$ nano platelets as building blocks to engineer a nano wire with *ABA* stacking. As shown in Figure 5c, although both platelets are metallic-like, the 3D wire is semiconducting and, thus, is an electric insulator. This is because of the fact that the metallic states in each single

layer of the platelets are mostly confined in the *xy* plane, and they do not overlap with each other in the *z* direction. However, when doping the wire by intercalating extra Mo atoms within the layers (see Figure 5e), a few energy bands appear across the Fermi level (see Figure 5f), thus making the new nano structure a metallic one. The dopant Mo atoms act as small "connectors" linking the metallic states of each platelets along the *z*-axis. The modification in the electronic structure along the *z* direction may result in a substantial increase in the electrical conductivity. It should be pointed out that the Mo−S nanowires composed of linear chains of $(Mo_3S_3)_n$ along the *z*-axis have been previously synthesized,[26] and they are also metallic.[27,28] However, the structure proposed here, as shown in Figure 5c, bears significant differences from the wires presented in ref 26; thus, it is expected to exhibit different properties. Assuming that Mo intercalation does not modify the expected low thermal conductivity of the wires, these nano-structures may become promising materials for thermoelectric applications. We note that multilayer MoS_2 nanoclusters can indeed be synthesized on a graphite surface.[29]

4. Conclusions

In summary, we have presented a study of the electronic properties of both 2D and 3D MoS_2 nano particles, and we have provided a unified interpretation of measured STM and photoluminescence spectra. In addition, our results indicate ways of engineering semiconducting 3D nanoparticles with direct band gaps and metallic nanowires that may have promising catalytic and thermoelectric properties.

References and Notes

(1) Lauritsen, J.; Kibsgaard, J.; Helveg, S.; Topsøe, H.; Clausen, B. S.; Lægsgaard, E.; Besenbacher, F. *Nat. Nanotechnol.* **2007**, *2*, 53.

(2) Hinnemann, B.; Moses, P. G.; Bonde, J.; Jørgensen, K. P.; Nielsen, J. H.; Horch, S.; Chorkendorff, I.; Nørskov, J. K. *J. Am. Chem. Soc.* **2005**, *127*, 5308.

(3) Jaramillo, T. F.; Jørgensen, K. P.; Bonde, J.; Nielsen, J. H.; Horch, S.; Chorkendorff, I. *Science* **2007**, *317*, 100.

(4) Chiritescu, C.; Cahill, D. G.; Nguyen, N.; Johnson, D.; Bodapati, A.; Keblinski, P.; Zschack, P. *Science* **2007**, *315*, 351.

(5) Chhowalla, M.; Amaratunga, G. A. *Nature* **2000**, *407*, 164.

(6) Rapoport, L.; Fleischer, N.; Tenne, R. *J. Mat. Chem.* **2005**, *15*, 1782.

(7) Helveg, S.; Lauritsen, J. V.; Lægsgaard, E.; Stensgaard, I.; Nørskov, J. K.; Clausen, B. S.; Topsøe, H.; Besenbacher, F. *Phys. Rev. Lett.* **2000**, *84*, 951.

(8) Bollinger, M. V.; Lauritsen, J. V.; Jacobsen, K. W.; Nørskov, J. K.; Helveg, S.; Besenbacher, F. *Phys. Rev. Lett.* **2001**, *87*, 196803.

(9) Bollinger, M. V.; Jacobsen, K. W.; Nørskov, J. K. *Phys. Rev. B* **2003**, *67*, 085410.

(10) Schweiger, H.; Raybaud, P.; Kresse, G.; Toulhoat, H. *J. Catal.* **2002**, *207*, 76.

(11) Lightstone, J. M.; Mann, H. A.; Wu, M.; Johnson, P. M.; White, M. G. *J. Phys. Chem. B* **2003**, *107*, 10359.

(12) Singh, D. M. D. J.; Pradeep, T.; Bhattacharjee, J.; Waghmare, U. V. *J. Phys. Chem. A* **2005**, *109*, 7339.

(13) Bertram, N.; Kim, Y. D.; Ganteför, G.; Sun, Q.; Jena, P.; Tamuliene, J.; Seifert, G. *Chem. Phys. Lett.* **2004**, *396*, 341.

(14) Bertram, N.; Cordes, J.; Kim, Y. D.; Ganteför, G.; Gemming, S.; Seifert, G. *Chem. Phys. Lett.* **2006**, *418*, 36.

(15) Seifert, G.; Tamuliene, J.; Gemming, S. *Comp. Mater. Sci.* **2006**, *35*, 316.

(16) Murugan, P.; Kumar, V.; Kawazoe, Y.; Ota, N. *J. Phys. Chem. A* **2007**, *111*, 2778.

(17) Wilcoxon, J. P.; Newcomer, P. P.; Samara, G. A. *J. Appl. Phys.* **1997**, *81*, 7934.

(18) Wilcoxon, J. P.; Samara, G. A. *Phys. Rev. B* **1995**, *51*, 7299.

(19) Baroni, S.; Corso, A. D.; de Gironcoli, S.; Giannozzi, P.; Cavazzoni, C.; Ballabio, G.; Scandolo, S.; Chiarotti, G.; Focher, P.; Pasquarello, A.; Laasonen, K.; Trave, A.; Car, R.; Marzari, N.; Kokaji, A. Plane-Wave Self-Consistent Field Home Page, http://www.pwscf.org.

(20) Vanderbilt, D. *Phys. Rev. B* **1990**, *41*, 7892.

(21) Marzari, N.; Vanderbilt, D.; De Vita, A.; Payne, M. C. *Phys. Rev. Lett.* **1999**, *82*, 3296.

(22) Tersoff, J.; Hamann, D. R. *Phys. Rev. B* **1985**, *31*, 805.

(23) Frindt, R. F.; Yoffe, A. D. *Proc. R. Soc. London, Ser. A* **1963**, *273*, 69.

(24) Yoffe, A. D. *Adv. Phys.* **1993**, *42*, 173.

(25) Mattheiss, L. F. *Phys. Rev. B* **1973**, *8*, 3719.

(26) Remskar, M.; Mrzel, A.; Skraba, Z.; Jesih, A.; Ceh, M.; Demšar, J.; Stadelmann, P.; Lévy, F.; Mihailovic, D. *Science* **2001**, *292*, 479.

(27) Meden, A.; Kodre, A.; Gomilšek, J. P.; Arčon, I.; Vilfan, I.; Vrbanic, D.; Mrzel, A.; Mihailovic, D. *Nanotechnology* **2005**, *16*, 1578.

(28) Gemming, S.; Seifert, G.; Vilfan, I. *Phys. Status Solidi B* **2006**, *243*, 3320.

(29) Kibsgaard, J.; Lauritsen, J. V.; Lægsgaard, E.; Clausen, B. S.; Topsøe, H.; Besenbacher, F. *J. Am. Chem. Soc.* **2006**, *128*, 13950.